Supplementary Material for

Evaluation of extreme temperature events as simulated by CMIP6 models over Central Africa

Gabriel Fotso-Kamga[1,2,*], Thierry C. Fotso-Nguemo[1,2,3], Zéphirin D. Yepdo[1,3], Alain T. Tamoffo[1,6], Zakariahou Ngavom[1,2], Sinclair Zebaze[1,4], Cyrille K. Kayimbo[7], Derbetini A. Vondou[1] and Arona Diedhiou[2,5]

[1]*Laboratory for Environmental Modelling and Atmospheric Physics (LEMAP), Department of Physics, Faculty of Science, University of Yaounde 1, P.O. Box 812 Yaounde, Cameroon*

[2]*Laboratoire Mixte International "Nexus Climat-Eau-Énergie-Agriculture en Afrique de l'Ouest et Services Climatiques" (LMI NEXUS), Université Félix Houphouët-Boigny, P.O. Box 463 Abidjan, Côte d'Ivoire*

[3]*Climate Change Research Laboratory (CCRL), National Institute of Cartography, P.O. Box 157 Yaounde, Cameroon*

[4]*Department of Earth and Atmospheric Sciences, Indiana University, Bloomington, IN, USA*

[5]*University of Grenoble Alpes, IRD, CNRS, Grenoble INP, IGE, 38000 Grenoble, France*

[6]*Climate Service Center Germany (GERICS), Helmholtz-Zentrum Hereon, Hamburg, Germany*

[7]*Research Unit of Industrial and Systems Engineering Environment (UR-ISIE), IUT/FV Bandjoun, University of Dschang, PO Box 134 Bandjoun, Cameroon*

Contents of this file

[*]**Corresponding author:** Gabriel Fotso-Kamga (kamga_fotso@yahoo.fr)

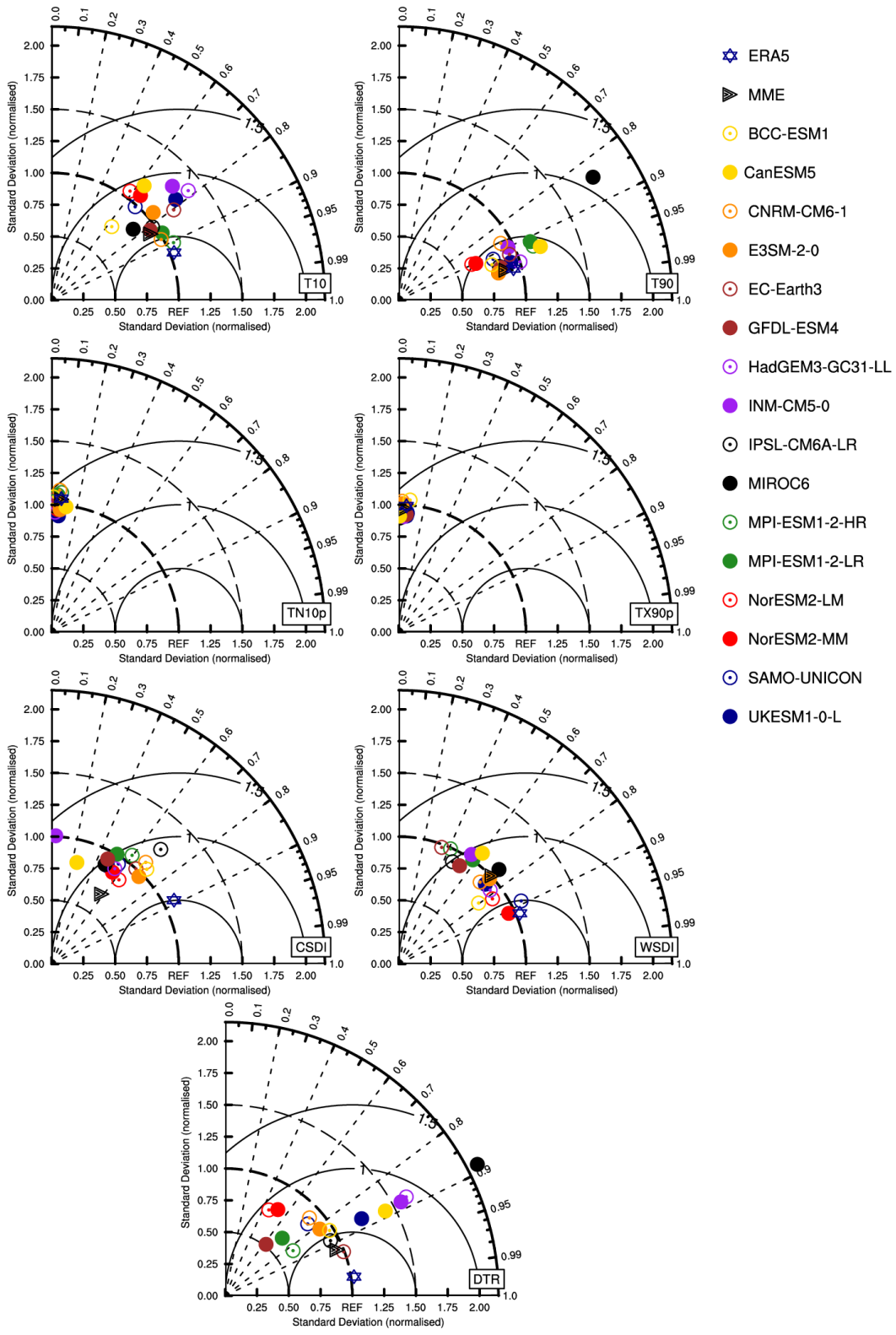

Fig. S1: Taylor diagram analysis showing the annual values for **a) percentile based indices** i.e., 90th percentile of maximum temperature (T90), 10th percentile of minimum temperature (T10), Warm days (TX90p) and Cool nights (TN10p); **b)** duration based indices i.e., Warm spell days index (WSDI) and Cold spell days index (CSDI); and **c) absolute based indice** i.e., Diurnal temperature range (DTR), derived from ERA5, MME and individual CMIP6 simulation members, averaged over the Central African domain, during the period 1985-2014. CHIRTS has been considered here as reference dataset

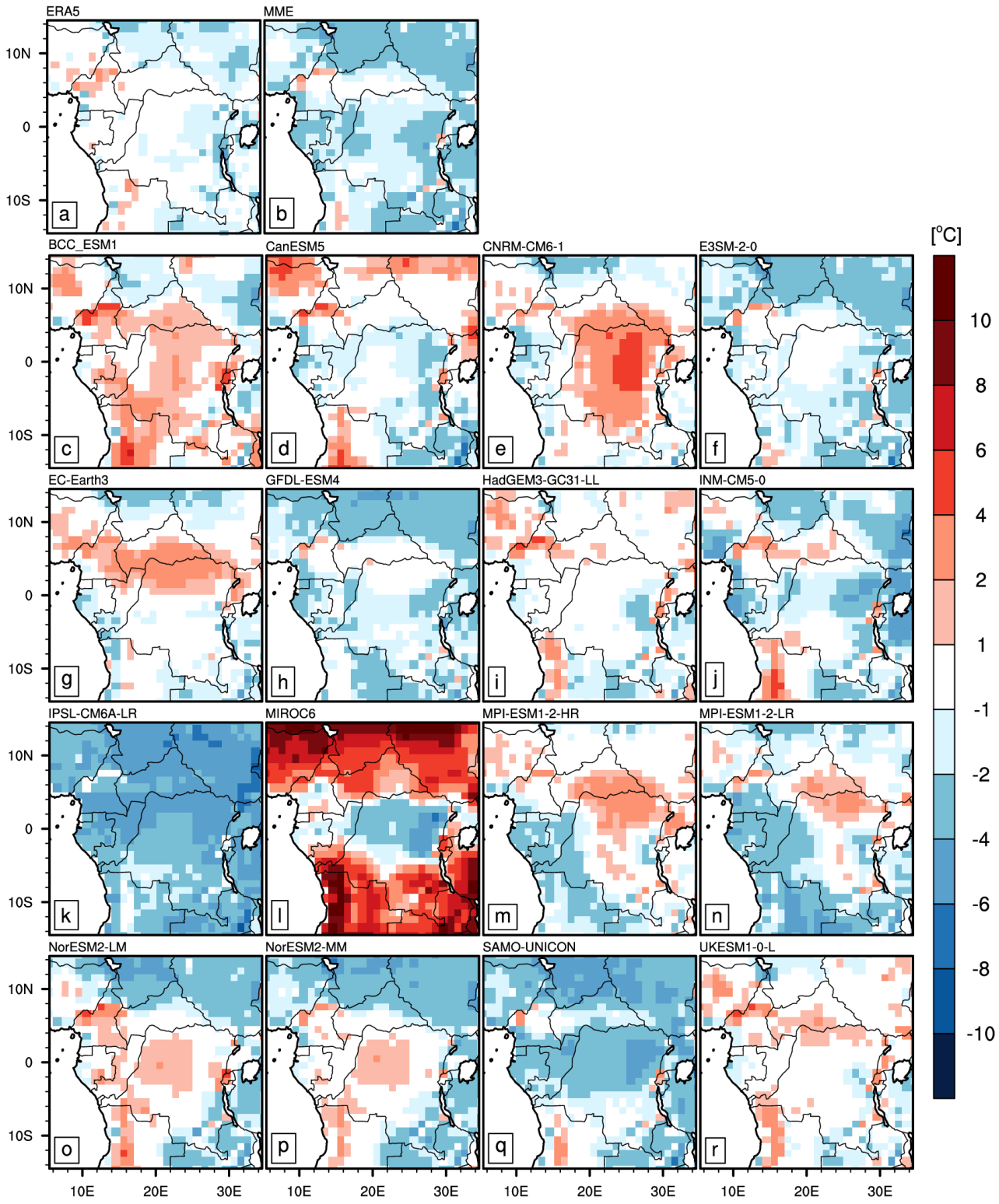

Fig. S2: Mean (1985–2014) spatial distribution of biases of the T90 (in °C), with respect to CHIRTS from a) ERA5, b) MME and c-r) individual CMIP6 simulation members.

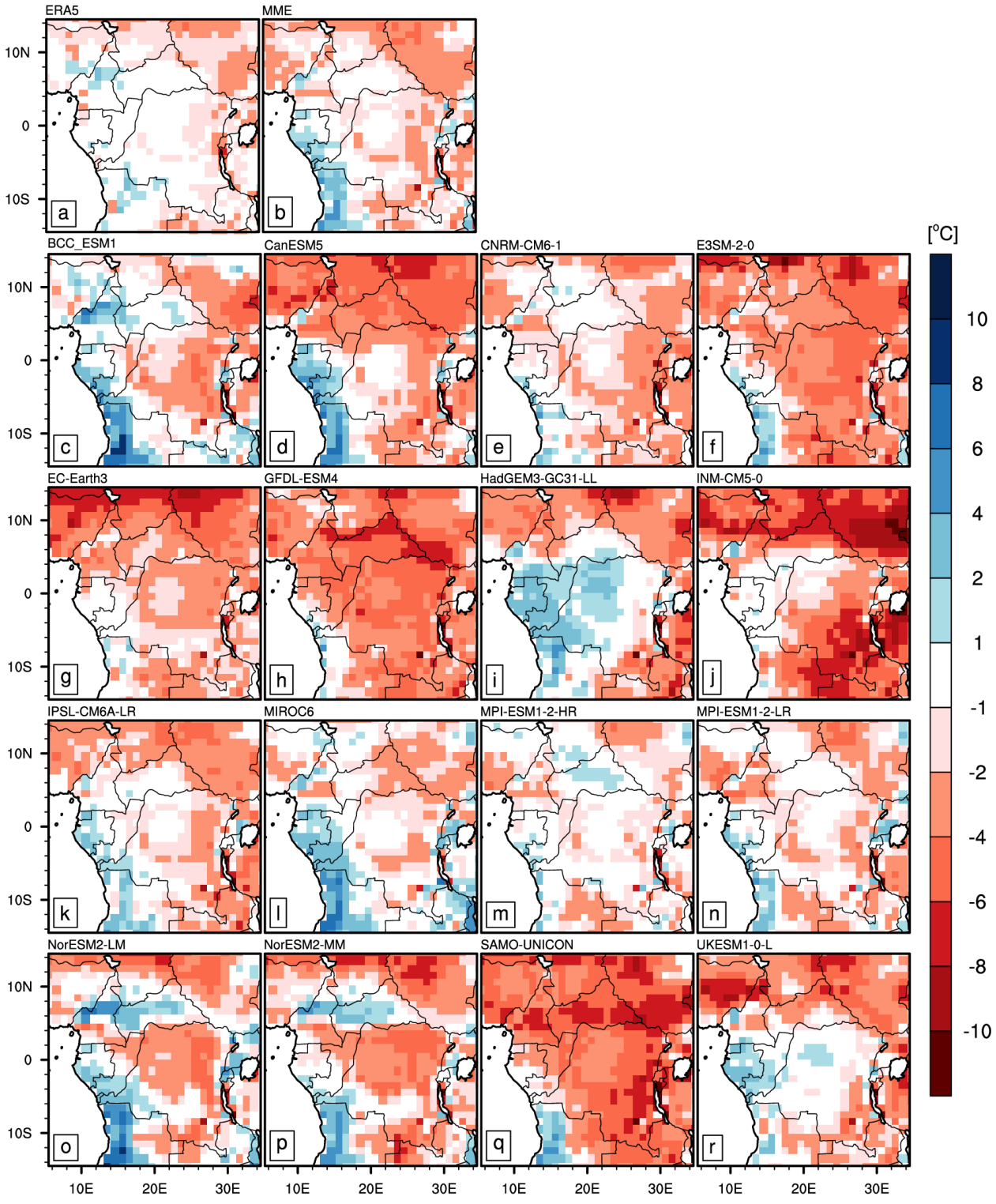

Fig. S3: Mean (1985–2014) spatial distribution of biases of the T10 (in °C), with respect to CHIRTS from a) ERA5, b) MME and c-r) individual CMIP6 simulation members.

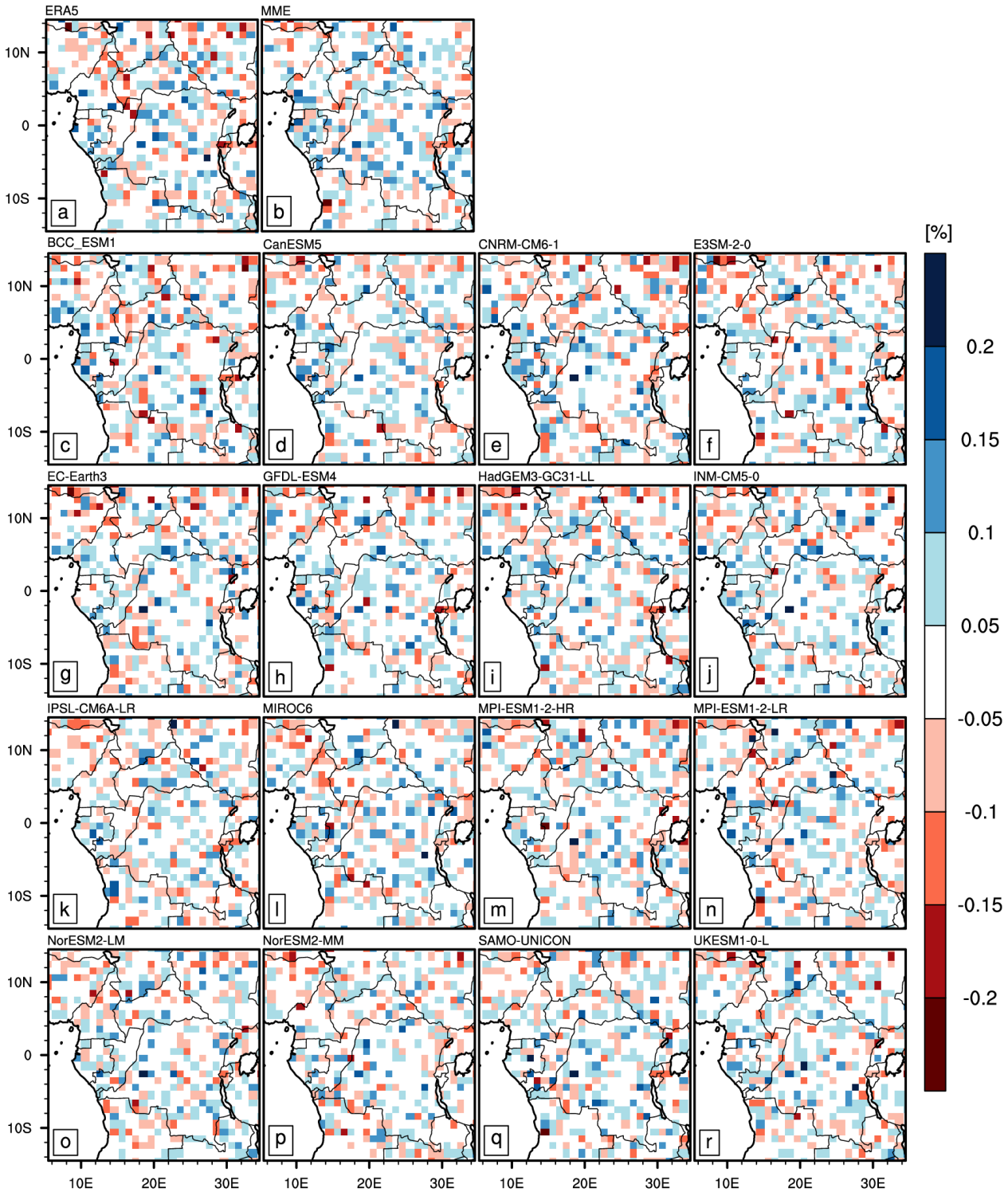

Fig. S4: Mean (1985–2014) spatial distribution of biases of the TX90p (in %), with respect to CHIRTS from a) ERA5, b) MME and c-r) individual CMIP6 simulation members.

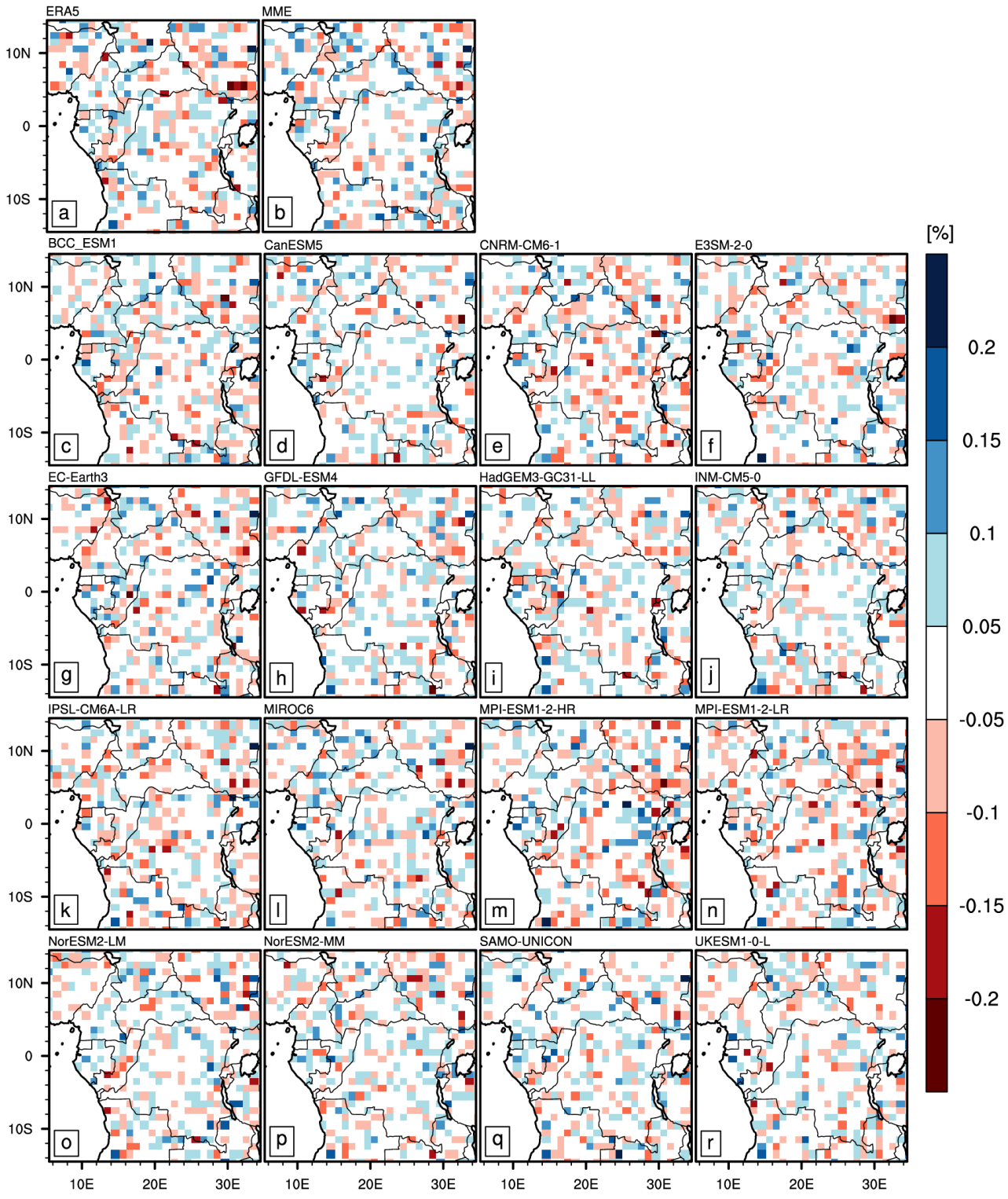

Fig. S5: Mean (1985–2014) spatial distribution of biases of the TN10p (in %), with respect to CHIRTS from a) ERA5, b) MME and c-r) individual CMIP6 simulation members.

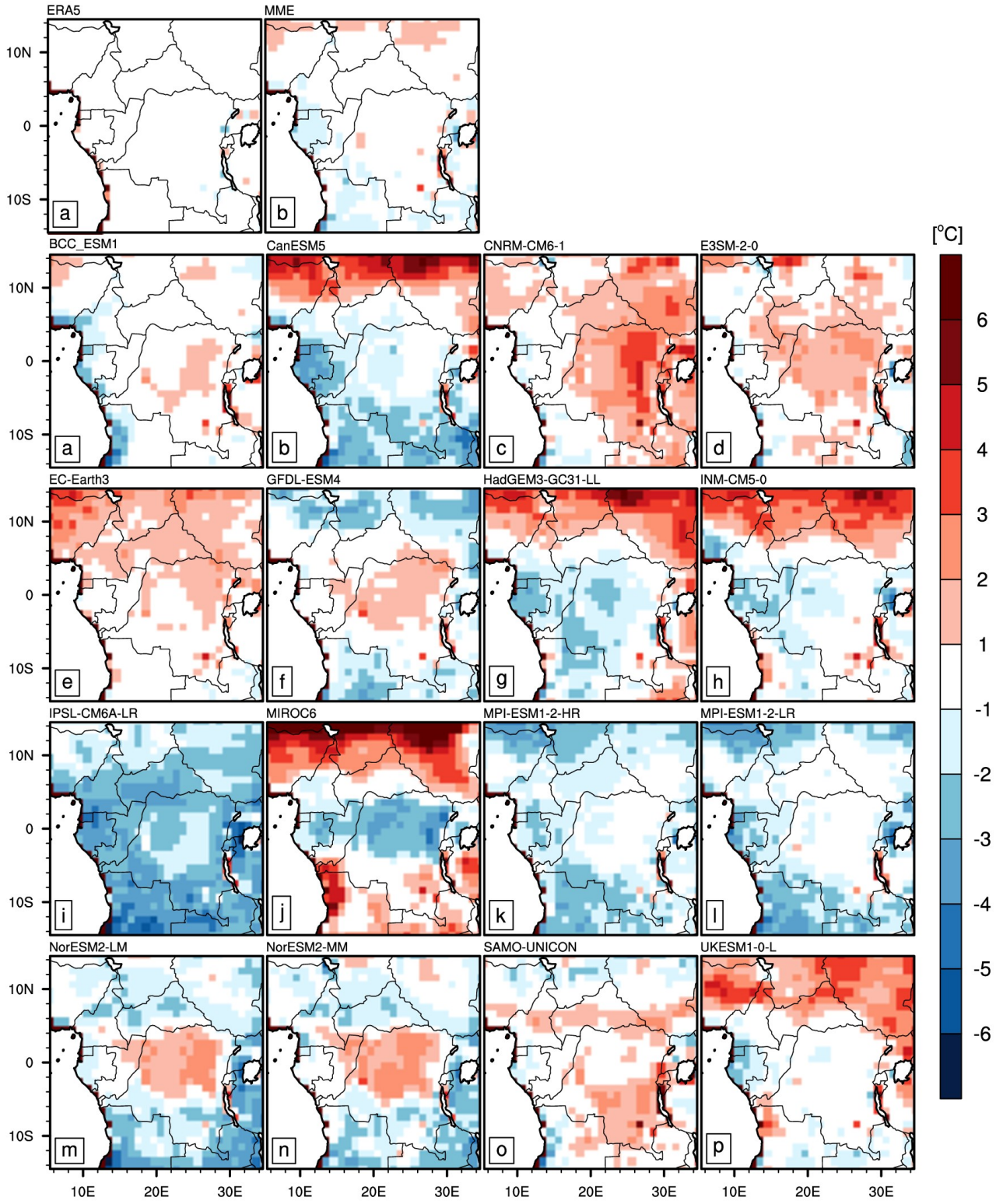

Fig. S6: Mean (1985–2014) spatial distribution of biases of the DTR (in °C), with respect to CHIRTS from a) ERA5, b) MME and c-r) individual CMIP6 simulation members.

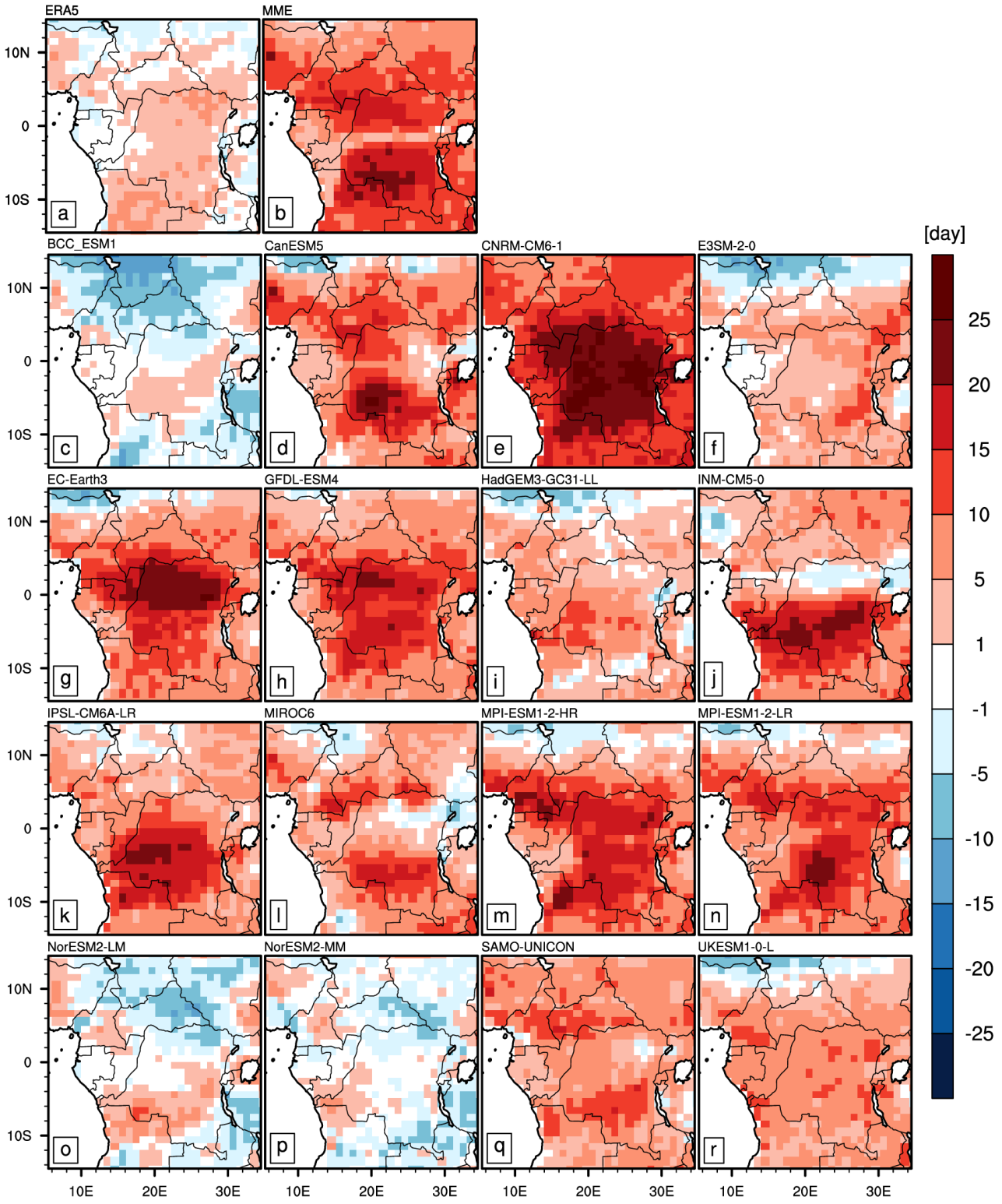

Fig. S7: Mean (1985–2014) spatial distribution of biases of the WSDI (in day), with respect to CHIRTS from a) ERA5, b) MME and c-r) individual CMIP6 simulation members.

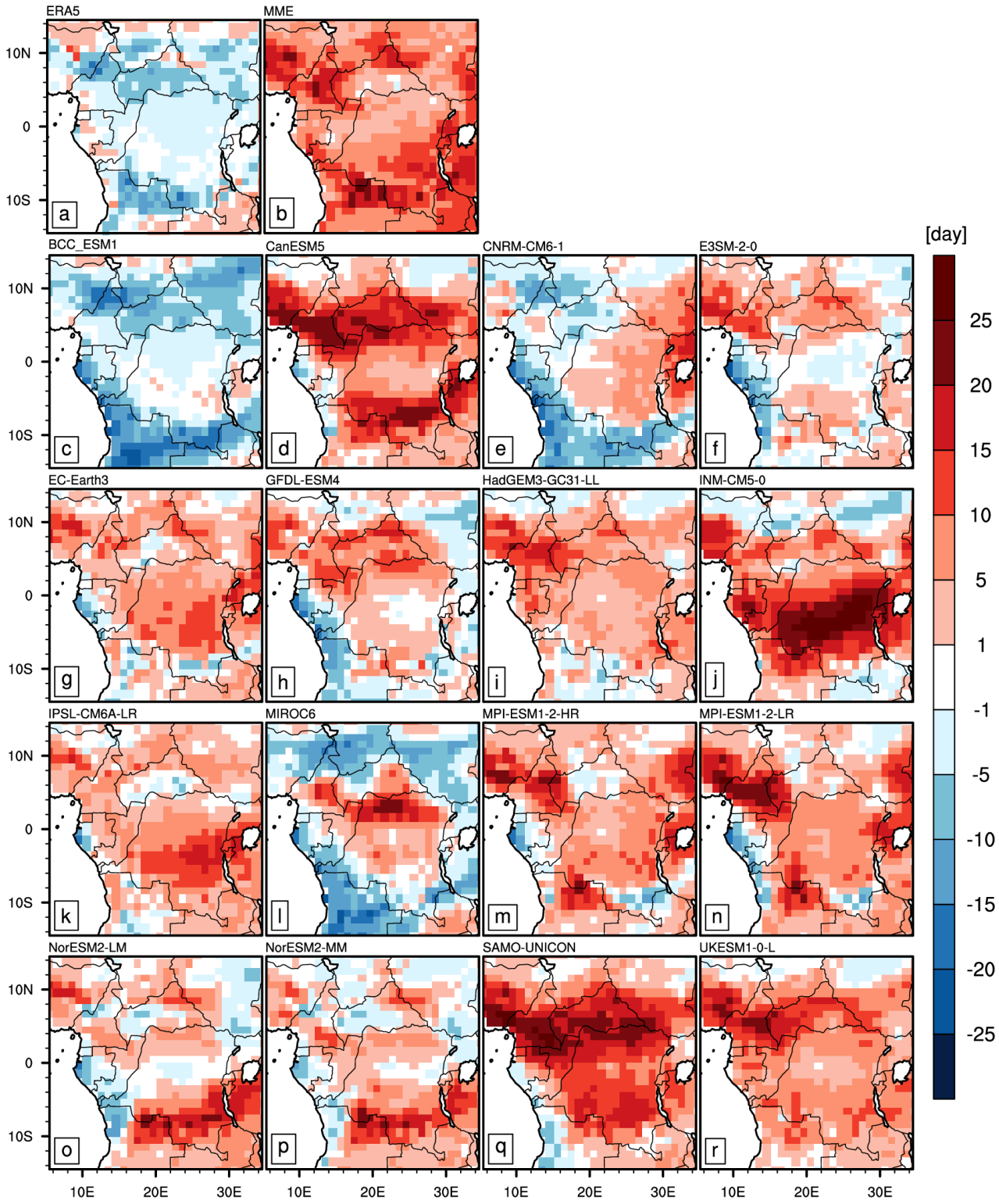

Fig. S8: Mean (1985–2014) spatial distribution of biases of the of the CSDI (in day), with respect to CHIRTS from a) ERA5, b) MME and c-r) individual CMIP6 simulation members.